SLIDING MODE CONTROL OF BRUSHLESS DC MOTOR SPEED WITH CHATTERING REDUCTION

J. R. B. A. Monteiro and C. M. R. Oliveira and M. L. Aguiar
School of Engineering of São Carlos
University of São Paulo
São Carlos, SP 13566-590
Email: jrm@sc.usp.br

***Abstract*—This paper proposes the use of an analog switching function in sliding mode control for a brushless DC motor speed, with the objective of input chattering reduction. The sliding mode control topology is used in the mechanical speed loop control as well as in the stator current loop control. The results show a good chattering reduction, a good machine performance and a good robustness of the controller due to disturbances, without the need of fine tunneling of the controller parameters, as in other kinds of control. The parameters of a real machine where used in the simulations. This kind of function in the used sliding mode controllers turned to be a very good alternative depending on the application.**

***Keywords*—sliding mode control, speed control, brushless DC motor, sliding mode chattering**

I. Introduction

It is undoubtedly that electrical machines are indispensable elements in contemporary world, from processes industry to home applications. Electrical motors have many advantages over other kind of motors, not limited to, but including: low cost, high power density, simple construction and installation requirements, robustness, versatility (it can be easily adapted to various types of loads), high efficiency and control simplicity [1].

Regarding the various types of electrical motors, direct-current motors are very attractive and widely used in variable speed applications. However, its brushes carry many of disadvantages, among then: the decrease of operational efficiency due to losses in the mechanical commutator and brushes themselves, high maintenance rate that increases machine operational cost, acoustic noise, electromagnetic noise due to brush spark, etc. Brushless DC motors, as it name says, do not have the disadvantages associated to brushes. Perhaps, their cost for equivalent machines are higher, but it tends to decrease over time, as electronics cost tends to decrease. However its main cost factor is due to the magnet material, which are high for high energy types. If the cost of such a machine is critical in an application, another kinds of machine can be used, as induction motors and switched reluctance motors [2].

II. Brushless DC Motor Electrical Drive

The therm brushless DC motor refers to the set composed by an electrical machine, more specifically a surface-mount permanent magnet synchronous machine, with its electric converter, commonly a three phase machine with a three phase electric converter (a three phase inverter) [3][4]. Ideally, the electrical machine has a trapezoidal back-EMF waveform and with a 120° square wave stator current produces an almost ripple free electromagnetic torque, as in Fig. 1. In this case, the converter operates in six-step mode and with each switch activated by 120° electrical, resulting in 2 switches activated simultaneously.

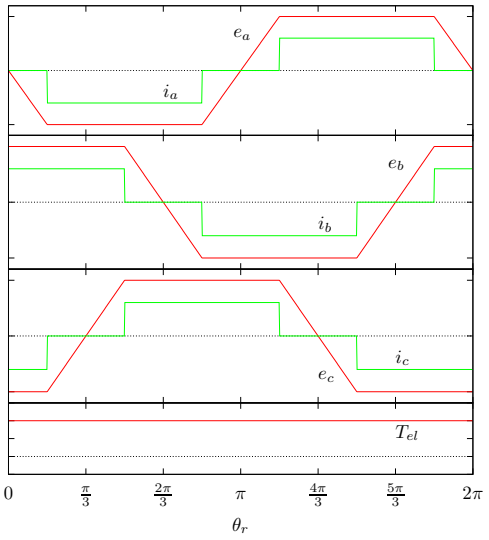

Fig. 1. Brushless DC motor ideal electromagnetic torque generation.

The machine model is shown in (1) to (5).

$$\begin{bmatrix} v_a \\ v_b \\ v_c \end{bmatrix} = \begin{bmatrix} L_s & M_s & M_s \\ M_s & L_s & M_s \\ M_s & M_s & L_s \end{bmatrix} \frac{d}{dt} \begin{bmatrix} i_a \\ i_b \\ i_c \end{bmatrix} + R_s \begin{bmatrix} i_a \\ i_b \\ i_c \end{bmatrix} + \begin{bmatrix} e_a \\ e_b \\ e_c \end{bmatrix} + \begin{bmatrix} v_n \\ v_n \\ v_n \end{bmatrix} \tag{1}$$

Where:

e_a, e_b and e_c: induced voltage of stator phases

a, b and c, respectively, due to rotor magnets movement, as in (2);
i_a, i_b and i_c: stator phase currents a, b and c, respectively;
L_s: stator phase self-inductance;
M_s: stator phases mutual inductances;
R_s: stator phase resistance;
v_a, v_b and v_c: a, b and c stator phases applied voltages, respectively;
v_n: stator neutral terminal voltage (this terminal is not normally connected).

$$\begin{bmatrix} e_a \\ e_b \\ e_c \end{bmatrix} = \frac{d}{dt} \begin{bmatrix} \Phi_{ra} \\ \Phi_{rb} \\ \Phi_{rc} \end{bmatrix} = \omega_e \begin{bmatrix} \Phi'_{ra} \\ \Phi'_{rb} \\ \Phi'_{rc} \end{bmatrix} \tag{2}$$

Where:

Φ_{ra}, Φ_{rb} and Φ_{rc}: linked magnetic fluxes between rotor magnets and stator winding phases a, b and c, respectively;
ω_e: electrical rotor speed.

$$T_e = n_{pp} \left(\Phi'_{ra} i_a + \Phi'_{rb} i_b + \Phi'_{rc} i_c \right) \tag{3}$$

Where:

T_e: machine-generated electromagnetic torque;
n_{pp}: number of machine's pole pairs;

As depicted in Fig. 1, the back-EMFs are ideally trapezoidal, therefore Φ'_{ra}, Φ'_{rb} and Φ'_{rc} are also trapezoidal as shown in Fig. 2, considering (2), where Φ_M is their amplitudes and θ_e is the rotor angle in electrical degrees.

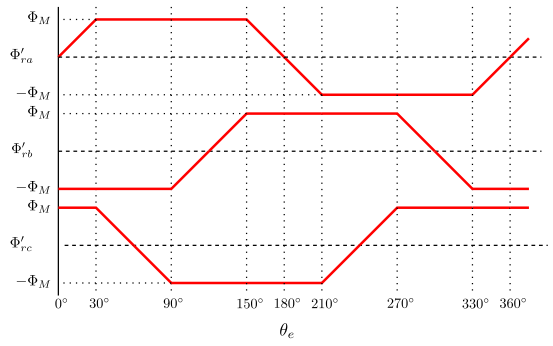

Fig. 2. Waveforms for Φ'_{ra}, Φ'_{rb} and Φ'_{rc}.

Eq. (1) can be also written as:

$$v_{abc} - [v_n] = R_s i_{abc} + (L_s - M_s) \frac{d}{dt} i_{abc} + e_{abc} \tag{4}$$

In order to produce a smooth electromagnetic torque in its shaft, the phase currents shown in Fig. 1 must be produced, so the inverter bridge (Fig. 3) must have only two switches closed each instant of time. Machine internal position sensors are responsible to signal to inverter bridge electronics which switches must be activated each time. Those sensors can be magnetic (by Hall effect) or optical, detecting rotor position in intervals of 60° electrical, in the case of a three-phase configuration. Taking into account (4) and negleting the effects of phase comutation, which lasts a fraction of time of phase conduction, the system can be reduced to Fig. 4, for simplified analysis purposes, which is similar to a four quadrant chopper.

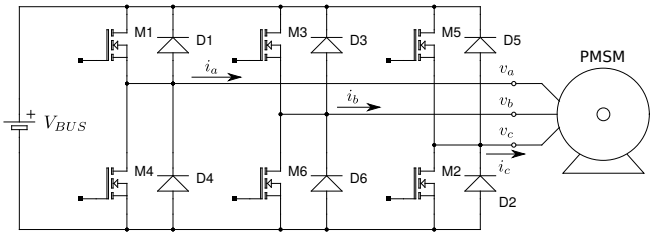

Fig. 3. Three-phase inverter bridge and PMSM machine.

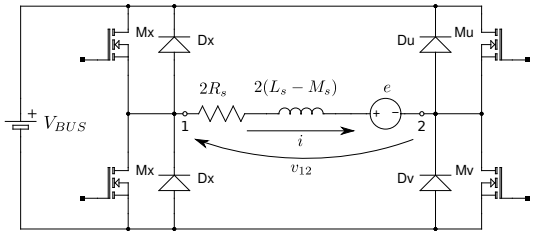

Fig. 4. Simplified BLDC motor equivalent circuit.

In Fig. 4, e is given by (5).

$$e = 2\Phi_M \omega_e \tag{5}$$

$$v_{12} = 2R_s\, i + 2(L_s - M_s) \frac{di}{dt} + 2\Phi_m \omega_e \tag{6}$$

Where:

v_{12}: voltage between terminals 1 and 2;
i: phase to phase current;

Depending on the signal from position sensors, transistor Mx (Fig. 4) can be M1, M3 or M5, My can be M2, M4 or M6; the same for Mu which can be M1, M3 and M5 and Mv can be M2, M4 or M6. The analogous for diodes Dx, Dy, Du and Dv. Eventually, terminals 1 and 2 can be any machine phase, a, b or c, each one.

As an example, supposing machine phase a is positive, phase b is negative and phase c is to be open, x=1, y=4, u=3, v=6, so Mx is M1, Dx is D1, My is M4, and so on. Terminal 1 is phase a and 2 is phase b.

Following, there are some different possibilities in order to obtain the desired voltage in machine terminals, to produce the goal current. It can be listed 3 of these possibilities, shown in Table I, where δ denotes that the PWM signal is applied to that switch, so it will be turned on during $\delta \cdot T$, where T is PWM period and δ is PWM duty cycle; 0 means the switch is off during all PWM period; 1 means switch in on; and $\bar{\delta}$ is the opposite of δ, which means the switch will be off during $\delta \cdot T$ and on the remaining PWM period time, i. e., $(1-\delta) \cdot T$.

TABLE I. SWITCHING SCHEMES USED TO FEED MACHINE PHASES.

Scheme	Mx	My	Mu	Mv
1	δ	0	0	δ
2	δ	0	0	1
3	δ	$\bar{\delta}$	0	1

The chosen scheme for this work is number 3, due to some advantages it presents over the others as it presents reduced current swing, it presents current continuous mode in any load and PWM duty cycle condition (which is not always true using numbers 1 and 2) and it is possible to regenerate energy (which is not in number 2).

A. Mechanical load

The dynamic mechanical load equation is shown in (7).

$$J\frac{d\omega}{dt} + B\omega + T_L = T_e \tag{7}$$

Where:

B: equivalent frictional coefficient, composed by rotor shaft bearings and load frictional losses;
J: combined inertia momentum of machine rotor and load;
T_L: load torque;
ω: rotor mechanical speed.

The machine parameters as well as mechanical load parameters are in Table II, load torque (T_L) is not show because it is different in each simulation.

TABLE II. BLDC MOTOR AND MECHANICAL LOAD PARAMETERS USED IN SIMULATIONS.

Motor	**Load**
$R_s = 2.3\Omega$	$J = 4.2 \cdot 10^{-3}\text{kg m}^2$
$(L_s - M_s) = 12.5\text{mH}$	$B = 3.032 \cdot 10^{-3}\text{kg m}^2/\text{s}$
$n_{pp} = 3$	
$\Phi_m = 0.12\text{Wb}$	

III. SLIDING MODE CONTROL

Sliding mode control was first presented to western World in a book published in 1976 [5] and, perhaps more known, a paper in 1977 [6]. The main idea in sliding mode control is once the sliding mode was reached, the system is immune to parametric variations and disturbances, limited to a sort of ranges, naturally.

In order to satisfy the conditions of convergence to the solution of the system, or the convergence to the sliding regime, it is necessary to define the sliding surface. The most used sliding surface is shown in (8) [7].

$$\sigma(x) = \left(\frac{d}{dt} + \lambda\right)^{r-1}(x^* - x) \tag{8}$$

Where:

r: is the degree of sliding surface;
x: vector of state variables;
x^*: references for state variables;
λ: weight factor.

In order to prove the convergence of a system like (9) one can write the system input function as (10), as it is a sum of a continuous function and a switching function.

$$\begin{aligned} \dot{x} &= f(x) + g(x)U \\ y &= h(x) \end{aligned} \tag{9}$$

Where:

U: system input;
f, g, h: linear or non-linear functions, characterizing the system;
y: system output.

$$U = U_{eq} + U_c \tag{10}$$

Where:

U_{eq}: is a continuous function and is referred as "equivalent control", representing the operation point where the sliding regime occurs [8];
U_c: is the switching control, representing the variable structure of the system, responsible to the attractiveness of the system to the sliding regime.

A well accepted method to prove the convergence of the system to the operation point is by the definition of V, a energy Lyapunov function:

$$V = \frac{1}{2}\sigma^2 \tag{11}$$

For the asymptotic stability of the chosen surface (8) in the equilibrium point ($\sigma = 0$), some conditions must be satisfied:
a) $\dot{V} < 0$ for $\sigma \neq 0$

b) $\lim_{|\sigma|\to\infty} V = \infty$

Condition b is clearly satisfied, but condition a follows:

$$\dot{V} = \sigma\dot{\sigma} \quad \text{and} \quad \dot{\sigma} = \frac{\partial\sigma}{\partial x}\dot{x} \tag{12}$$

Writing (9) using the defition of the input as in (10):

$$\dot{x} = (f(x) + g(x)U_{eq}) + (g(x)U_c) \tag{13}$$

Solving U_{eq} to make the first therm of (13) be zero or, in other way, from the definion of equivalent control as the portion of control that is responsible for the set point of the system:

$$U_{eq} = -\left(\frac{\partial\sigma}{\partial x}g(x)\right)^{-1}\left(\frac{\partial\sigma}{\partial x}f(x)\right) \tag{14}$$

Rewritten (12) using above:

$$\dot{V} = \sigma\dot{\sigma} = \sigma\frac{\partial\sigma}{\partial x}g(x)U_c < 0 \tag{15}$$

A simple form of implementing U_c is by signal function (16), however it causes a drawback in system performance due to the so called chattering, which can be considered the main drawback of sliding mode control [9]. But the purpose of the use of signal function in this section is to show the convergence by proving (15) inequality.

$$U_c = \rho\,\text{sign}(\sigma(x)) \tag{16}$$

Where:

ρ: amplitude of switching control input.

Considering the use of function sign in (15):

$$\dot{V} = \frac{\partial S}{\partial x}g(x)\rho\,|\sigma(x)| < 0 \tag{17}$$

As the therm $\rho\,|\sigma(x)| > 0$, then the stability of the system depends on the internal product of the surface σ partial derivative by x by the function $g(x)$:

$$\frac{\partial\sigma}{\partial x}g(x) < 0 \;\text{ for }\; \sigma \neq 0 \tag{18}$$

Following section assesses the stability for each considered control system.

IV. Proposed Topology

The control system diagram is shown in Fig. 6, where G_I represents the current loop controller and G_ω represents the speed loop controller. As the time constant of mechanical system is far greater than time constant of electrical system, it is possible to make separate analysis for the controllers of speed loop (G_ω) and for current loop (G_I) [10].

For the current control loop, (6) must be written in the form of (9) in order to verify if it satisfies (18), as in (19). Also, the equivalent control expression has solution considering the range for shaft speed operation and maximum stator current (20).

$$\frac{\partial\sigma_I}{\partial i}g_I(i) = -\frac{1}{2(L_s - M_s)} < 0 \tag{19}$$

$$\delta_{eq} = 2\frac{R_s + \Phi_M\omega_e}{V_{BUS}} \tag{20}$$

Where $\sigma_I = i^* - i$.

The same for speed control loop, where (7) must be written in the form of (9) to verify if it satisfies (18), as in (21). Additionally, the equivalent control expression has solution considering load torque and shaft speed operational ranges.

$$\frac{\partial\sigma_\omega}{\partial\omega}g_\omega(\omega) = -\frac{1}{J} < 0 \tag{21}$$

$$T_{e_{eq}=} = B\omega + T_L \tag{22}$$

Where $\sigma_\omega = \omega^* - \omega$.

As condition (18) is satisfied for both control loops, is time to define each one. For the speed controller G_ω follows:

$$T_e^* = T_{eM}\tanh k_\omega \cdot \sigma_\omega \tag{23}$$

Where:

T_e^*: electromagnetic torque reference;
T_{eM}: maximum allowed electromagnetic torque for this particular machine;
k_ω: hyperbolic tangent constant, it defines the inclination of hyperbolic tangent;
ω^*: shaft rotor speed reference.

Regarding to the diagram of Fig. 6, the saturation block for $i^{*\prime}$ is unnecessary, as T_e^* from (23) has its maximum and minimum values limited by tanh, but it can be maintained for sake of security, in the case of an implementation.

Now, for the current controller G_I:

$$\delta = \tanh k_I \cdot \sigma_I \tag{24}$$

Where:

δ: PWM duty cycle, as stated before, with the difference that here it can be a negative number, which means machine will be fed in the opposite direction[1];
k_I: hyperbolic tangent constant for current.

One must note that the use of tanh in the place of sign does not alter condition (18), once the therm $\sigma\tanh\sigma$ is positive for $\sigma \neq 0$.

Fig. 5 shows the effect of some tanh coefficients in order to better illustrate tanh as a signal function, where it is seen that for higher values of k, it behaves close to a sign function ($k = 100$); in the opposite, it resembles a line ($k = 1$).

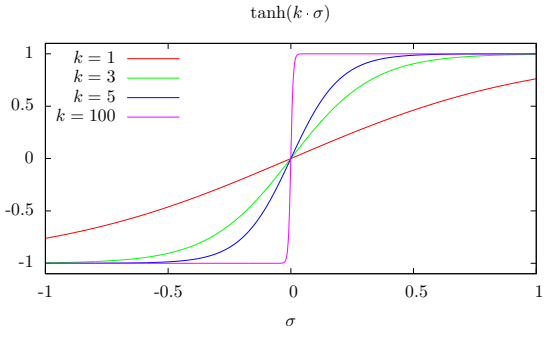

Fig. 5. Some tanh coefficient examples.

[1] In practice, the position sensors signals are going to be inverted, so machine will be fed by a "negative" voltage by the inverter bridge, or in other therms, the voltage is displaced by 180° electrical.

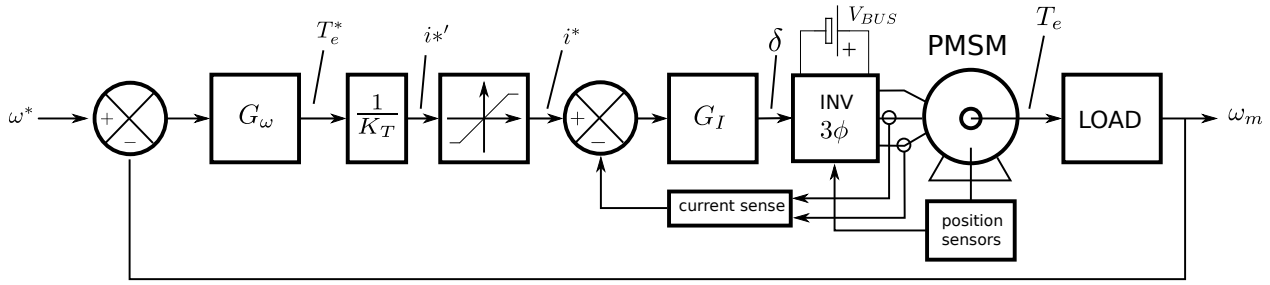

Fig. 6. System crontrol diagram.

With the help of Fig. 5, it is possible to pick up k for each controller, so:

$$k_\omega = \frac{k}{\omega_M} \quad \text{and} \quad k_I = \frac{k}{I_M} \tag{25}$$

Where:

ω_M: is the maximum shaft speed;
I_M: is the maximum stator current allowed to the machine, which is matched to its maximum electromagnetic torque.

The used values for the simulations are $k_\omega = 5$ and $k_I = 3$ and, for machine, $\omega_M = 2000\text{rpm}$ and $T_M = 3.6\text{N.m}$ ($I_M = 5\text{A}$).

V. Results

The starting operation of BLDC motor is shown in Fig. 7, where it accelerates up to 1000 rpm (104.7rd/s), with no load torque until $t = 0.15\text{s}$, after that, load torque of 2.2N.m (machine nominal load) is applied in its shaft. It can be seen that a low speed error is present after that instant and it is equal to 0.55rd/s (0.52% of error).

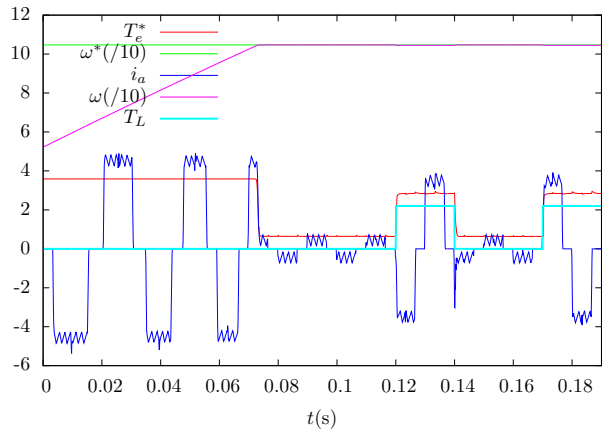

Fig. 7. BLDC motor starting with proposed SMC using tanh function as analog sign function.

Fig. 8 shows the acceleration of BLDC motor up to 2000rpm (209.4rd/s), with some shaft torque load variations, as shown in the figure. The final machine rotor speed is 209.4rd/s, an error of 0.4rd/s (0.2% of error).

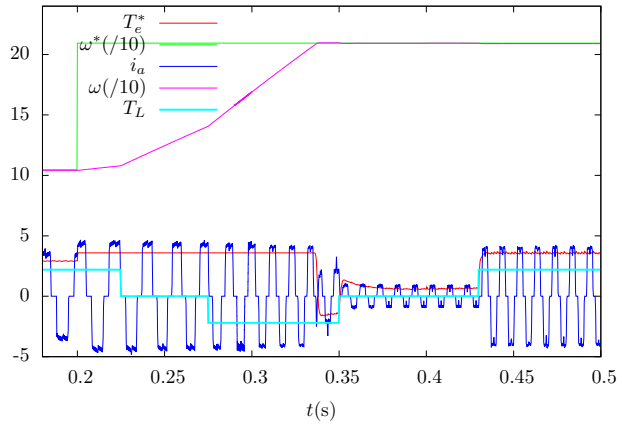

Fig. 8. BLDC motor with proposed SMC using tanh function as analog sign function.

Fig. 9 shows the reversion of the machine, from 2000rpm to -2000rpm. During the reversion, the mechanical load is applied in different directions. After 0.4s, the maximum torque allowed to the machine is 5N.m, so the machine has an extra torque to accelerate.

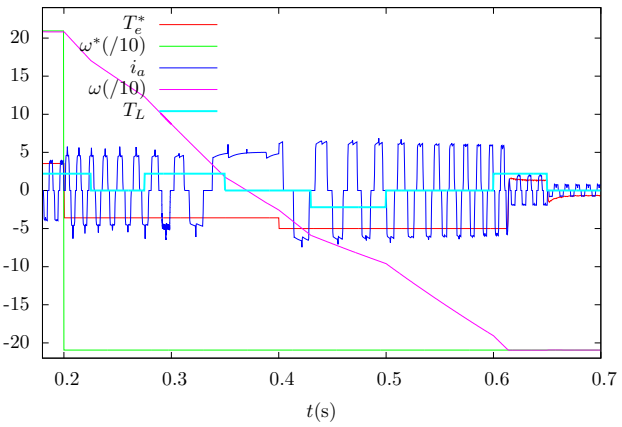

Fig. 9. BLDC motor during reversion with proposed SMC using tanh function as analog sign function.

And in Fig. 10, a zoom in the interval from 0.6s to 0.7s shows machine regenerating power to its source, the DC bus, in this case. It is possible to see the PWM duty cycle reference, which is the output of the controller G_I, where it presents a

very low level of chattering.

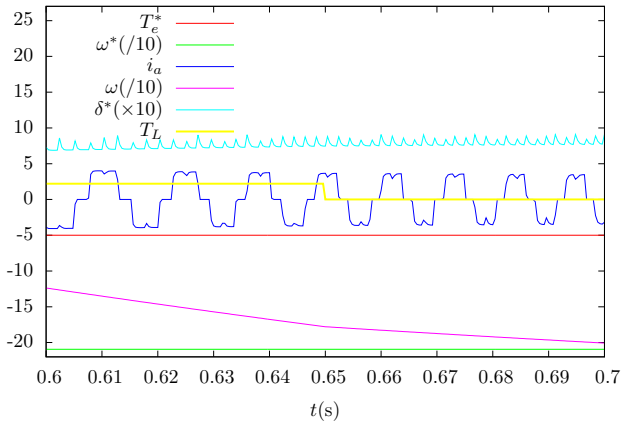

Fig. 10. BLDC motor regenerating energy to its power source.

The phase plane considering the machine operation shown in Fig. 7 is shown in Fig. 11, where it can be seen that speed error due to shaft load variation can reach about 2rpm (when machine achieves its set point at aprox. 1000rpm), and the error due to machine parameters variation are neglivible, as shown by other curves (colors other than red). In Fig. 12, it is shown the same load operational conditions of the previous Fig., except that k_ω is now equal to 3. It can be seen that load variation is still the major factor causing speed error (about 5rpm) but machine parameters variation plays a noticeable role when operating at full load.

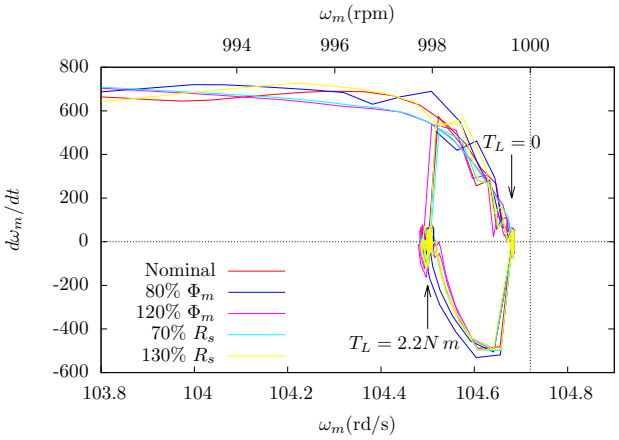

Fig. 11. Phase plane for BLDC motor operating at 1000rpm under load and machine parameters variations, using $k_\omega = 5$.

VI. Conclusions

The use of SMC has some advantages as it is very robust to plant parameter variation, to external disturbances and uncertainties. Also, it can be pointed out the low effort by the designer to tunneling controller parameters, as is the case of this work.

The use of hyperbolic tangent, instead of the signal function for sliding mode control topology, in BLDC motors also proved to be robust and with some advantages over the signal

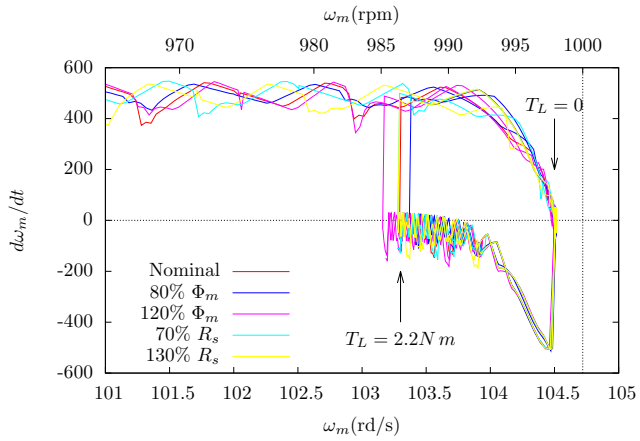

Fig. 12. Phase plane for BLDC motor operating at 1000rpm under load and machine parameters variations, using $k_\omega = 3$.

function, as the reduction of chattering in its input, i. e., in the electromagnetic torque reference, considering the speed controller, and the PWM duty cycle, considering the current control loop. One drawback that can be pointed out concerns the steady state error presented in the results for shaft speed, but it can be neglected depending on the application due to its low value, around 0.5%. Considering this error, it is presented by the system only under full load torque, but it can be considered imperceptible in major part of applications of this nature.

Acknowledgment

The authors would like to acknowledge FAPESP and CAPES for the financial support given to this research.

References

[1] A. Fitzgerald, C. Kingsley, and S. Umans, *Electric Machinery*, ser. Electrical Engineering Series. McGraw-Hill Companies,Incorporated, 2002.

[2] A. Vagati, A. Fratta, G. Franceschini, and P. Rosso, "AC motors for high-performance drivers: A design-based comparision," *IEEE Transactions on Industry Applications*, vol. 32, no. 5, 1996.

[3] S. A. Nasar, I. Boldea, and L. E. Unnewehr, *Permanent magnet, relutance, and self synchronous motors*. Boca Raton: CRC Press, 1993.

[4] T. J. E. Miller, *Bushless Permanent-Magnet and Reluctance Motor Drives*. Oxford: Claredon Press, 1993.

[5] U. Itkis, *Control Systems of Variable Structure*. Whiley, 1976.

[6] V. Utkin, "Variable structure systems with sliding modes," *Automatic Control, IEEE Transactions on*, vol. 22, no. 2, pp. 212–222, Apr 1977.

[7] J. Slotine and W. Li, *Applied nonlinear control*. Englewood Cliffs: Prentice Hall, 1991.

[8] M. Mahmoudi, N. Madani, M. Benkhoris, and F. Boudjema, "Cascade sliding mode control of a field oriented induction machine drive," *The European Physical Journal Applied Physics*, vol. 7, pp. 217–225, 1999.

[9] K. Young, V. Utkin, and U. Ozguner, "A control engineer's guide to sliding mode control," *Control Systems Technology, IEEE Transactions on*, vol. 7, no. 3, pp. 328–342, May 1999.

[10] B. M. Patre, V. M. Panchade, and R. M. Nagarale, *Sliding Mode Control*. InTech, 2011, ch. Sliding Mode Control of DC Drives, available from: http://www.intechopen.com/books/sliding-mode-control/sliding-mode-control-of-dc-drives.